ELSEVIER

28 July 1997

PHYSICS LETTERS A

Physics Letters A 232 (1997) 299–304

Investigation of the coupling between the outer electrodes in the superconducting double-barrier devices

I.P. Nevirkovets [a,1], J.E. Evettes [a], M.G. Blamire [a], Z.H. Barber [a], E. Goldobin [b]

[a] *Department of Materials Science and Metallurgy, University of Cambridge, Pembroke Street, Cambridge CB2 3QZ, UK*

[b] *Institute for Radio Engineering and Electronics of the Russian Academy of Sciences, Mokhovaya Street 11, Moscow 103907, Russian Federation*

Received 13 February 1997; revised manuscript received 12 May 1997; accepted for publication 16 May 1997
Communicated by J. Flouquet

Abstract

It is found experimentally that the critical current in the two-terminal double-barrier Nb/Al–AlO_x–Nb/Al–AlO_x–Nb device is considerably larger than the critical current in the bottom junction of the Nb/Al–AlO_x–Nb/Al–AlO_x–Ta/Nb device of identical planar configuration produced in the same deposition run. Our data suggest that the origin of the phenomena is a direct Josephson coupling between the external electrodes rather than the inductive interaction between the junctions. © 1997 Elsevier Science B.V.

PACS: 74.50.+r
Keywords: Stacked junctions; Josephson effect; Supercurrent enhancement

1. Introduction

Recently, much attention has been paid to physical properties and applications of stacked Josephson devices [1–3]. So far, the theoretical description of the stacked structures is limited to the inductive coupling between the junctions in the stack [1], which is valid if the condition $d < \lambda_L$ is satisfied (here d is the spacing between the junctions, λ_L is the London penetration depth).

However, new effects may appear if the middle superconducting layer becomes very thin: $d \sim \xi$, where ξ is the coherence length in the superconductor. Such a situation is realized, for example, in naturally layered high-temperature superconductors [4], and, in some respects, can be modelled in Nb-based structures [5].

The interference of the wave functions of the Josephson junctions separated by a distance $l \sim \xi$, is known to occur in the planar structures with direct conductivity of the junctions and leads to a strong interaction between them [6]. The interaction is essentially a nonequilibrium effect caused by concentration of the current passing through the constriction, where its magnitude exceeds the Ginzburg–Landau depairing current. The situation is different for tunnel junctions, in which there is no nonequilibrium in the stationary state. On the other hand, since all the types of Josephson junctions behave similarly in all the basic respects [7], one might expect that

[1] Permanent address: Institute for Metal Physics, National Academy of Sciences of the Ukraine, Vernadsky Blvd. 36, UA-252680 Kiev 142, Ukraine. E-mail: ipn@d24imp.kiev.ua.

PII S0375-9601(97)00388-5

additional coupling appears in vertically integrated tunnel structures with very thin superconducting layers between the tunnel barriers.

In this paper we present the results of an experiment intended to verify for the first time the presence of a direct weak coupling between the external electrodes in a double-barrier tunnel device with a thin middle superconducting layer.

2. Experiment

The double-barrier devices were fabricated from the Nb/Al–AlO_x–Nb/Al–AlO_x–Nb (type one) and Nb/Al–AlO_x–Nb/Al–AlO_x–Ta/Nb (type two) structures deposited in the same vacuum run. The fabrication route is essentially the same as that described elsewhere [3,8]. Deposition of both structures and oxidation of the barriers have been performed simultaneously under the same conditions up to the second tunnel barrier. After formation of the second barrier, one half of the substrates was screened by a shutter and Ta was deposited on the rest of the substrates. Then the shutter was opened and a Nb counterelectrode was deposited on all the substrates. Thus we have obtained structures identical in all the respects except the different counterelectrode. The parameters of the films as deposited are as follows: $d_1 = 150$ nm, $d_2 = 4$ nm, and $d_3 = 130$ nm are the thicknesses of the bottom, middle, and top Nb films, respectively; $d_{Al} = 5$ nm is the thickness of each Al layer, and $d_{Ta} = 40$ nm is the thickness of Ta film.

The two-terminal devices of the same geometry have been fabricated from each type of structure. Fig. 1 shows schematically the configuration of the Nb/Al–AlO_x–Nb/Al–AlO_x–Nb and Nb/Al–AlO_x–Nb/Al–AlO_x–Ta/Nb devices. The devices are square-shaped with the area in the plane 9×9 μm^2. Both top and bottom junctions have approximately equal specific tunnel resistances of order 10^{-6} Ω cm^2 and Josephson critical current densities (for the Nb/Al–AlO_x–Nb junctions) of order 1 kA/cm^2 at $T = 4.2$ K. The ratio of the subgap resistance at the voltage $V = (\Delta_1 + 2\Delta_2 + \Delta_3)/2e$ (where Δ_1, Δ_2, and Δ_3 are superconducting energy gaps of the bottom, middle, and top superconducting Nb layers, respectively) to the resistance well above

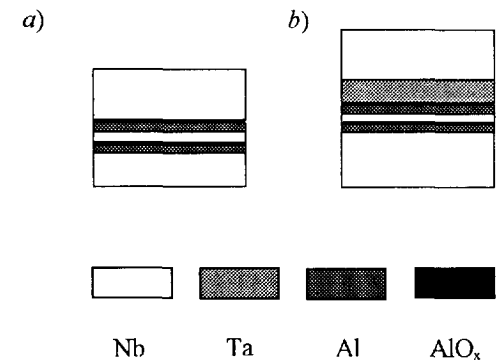

Fig. 1. Schematical cross-sectional view of the Nb/Al–AlO_x–Nb/Al–AlO_x–Nb (a) and Nb/Al–AlO_x–Nb/Al–AlO_x–Ta/Nb (b) devices.

the gap sum voltage is approximately equal to 9 at $T = 4.2$ K. This is a reasonably good value taking into account that the thin middle layer has a reduced superconducting transition temperature $T_c = 6.3$ K.

3. Results and discussion

Current–voltage characteristics (IVCs) of the planar arrays consisting of seven double-barrier devices connected in series are shown in Fig. 2. Curves for type 1 and type 2 devices are marked by squares (curve 1) and circles (curve 2), respectively. At successive voltages, the IVCs reveal the fine step structure which is due to the transition into the resistive state of the single junctions from the array.

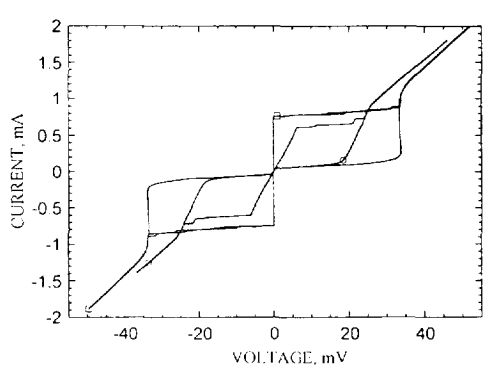

Fig. 2. Current–voltage characteristics of the series arrays consisting of double-barrier type 1 (boxes) and type 2 (circles) devices. The arrow shows the feature related with the gap difference $n(\Delta_{Nb} - \Delta_{Ta})$ of the Nb/Al–AlO_x–Nb/Ta junctions.

On the expanded scale, this allows one to determine the critical current values for the single junctions. For type 1 devices, the critical currents averaged over the two opposite directions of the bias current for the array shown in Fig. 2 (curve 1) are in the range from 749 to 882 μA. Here we suppose that the nth step for the positive bias current and the nth step for the negative bias current are for the same junction. The average critical current value (for 14 junctions in the array) is $I_c = 803$ μA. We could not distinguish the critical currents of the top and bottom junctions because they are very close to each other.

Now we consider the curve 2 in Fig. 2. It is the sum of IVCs of Nb/Al–AlO_x–Nb/Al and Nb/Al–AlO_x–Ta/Nb junctions. Since the superconducting transition temperature of Ta film is only slightly above $T = 4.2$ K, the IVC of the top junction has a shape close to that of the SIN junction. The bottom Nb/Al–AlO_x–Nb/Al junction is a SIS-type junction. So the total IVC of the device has the shape of a "twisted" Josephson junction. It is seen from the plot that the critical currents of 6 junctions perfectly coincide with each other, while the 7th junction has slightly larger critical current (there is a small step from this junction near the gap-sum voltage). The averaging procedure described above gives for the critical currents of 7 bottom junctions of this array the range from 606 to 717 μA. The average value of the critical current is $I_c = 640$ μA.

Both the visual comparison of the curves 1 and 2 in Fig. 2 and critical current values derived from them above clearly demonstrate the difference in supercurrent through the bottom junction of type 2 devices and type 1 devices. In fact, the average value of I_c of the Nb/Al–AlO_x–Nb/Al junctions of type 2 devices is about 20% smaller than that of the Nb/Al–AlO_x–Nb/Al–AlO_x–Nb devices. We believe this difference is of physical, rather than technological, origin. The bottom Nb/Al–AlO_x–Nb/Al junction in the type 2 devices is identical to the bottom junction in the type 1 devices. Although the type 1 and type 2 devices were fabricated on different chips, our experience shows that the critical current of the junctions is highly reproducible for the chips prepared in the same vacuum run. The spread of I_c values for different chips does not exceed the spread of I_c values within a single chip.

We should analyze a possible influence of parasitic effects which may be responsible for a reduced critical current of the bottom junction in type 2 devices. One effect might be heating: one can suppose that power dissipated in the device due to the bias current is larger for type 2 devices as compared with type 1 devices. To produce a critical current reduction by 20%, the energy gap of the superconducting electrodes should be reduced by an amount of the same order of magnitude. However, as can be seen from Fig. 2, the total gap-sum voltage of Nb/Al–AlO_x–Nb junctions in type 2 devices $V_g = n(\Delta_1 + \Delta_2)/e$ (here $n = 7$ is the number of devices connected in series) obtained from curve 2 is equal to $0.5V_{gNb} = n(\Delta_1 + 2\Delta_2 + \Delta_3)/e$, where V_{gNb} is the total gap-sum voltage obtained from curve 1. Therefore, even if heating affects the IVC, the effect is small and equal for both types of devices. Hence, the heating should be ruled out as an explanation of the phenomena.

Second, one should take into account possible inhomogeneous current distribution over the area of the type 2 device. As a result, the total critical current through the bottom junction might be reduced as compared with the magnitude of I_c through the type 1 device, because of the shorter Josephson penetration depth λ_J in the first case. Such an effect occurs in the devices with very thin middle layer [3], even if the lateral dimensions of the device are a few tens of μm. The analysis of the experimental data in our case would be much simpler if the Ta layer had a thickness large enough for the proximity effect to be neglected. However, the temperature dependence of IVC of type 2 devices shows that the $\Delta_{Nb} - \Delta_{Ta}$ gap-difference feature persists up to the temperature $T_{NSc} \approx 6.0$ K, which is above the equilibrium critical temperature of bar Ta, $T_c = 4.5$ K. Such a behavior reveals the proximity effect in the Ta/Nb bilayer. Quantitative analysis of the effective magnetic penetration depth of the proximity bilayers is quite complicated [9,10] and is beyond of the scope of this paper. However, the available experimental data allow one to draw a correct, to our belief, qualitative conclusion. It is known that the screening length in the normal metal being a part of the N/S proximity bilayer is $\lambda_N(x, T)^{-1} \propto \Delta_N(x, T)$ [11], where Δ_N is the energy gap induced in N, x is the coordinate perpendicular to the N/S interface ($x = 0$ at the free surface of the N layer). Since at the temperature

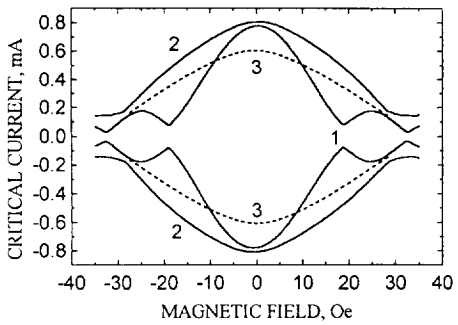

Fig. 3. The $I_c(H)$ dependences for the type 1 and type 2 devices. Curve 1 is the $I_c(H)$ dependence of the critical current at which the type 1 device as a whole switches to the resistive state, curve 2 is for the critical current of the single junction in the same device, when the second junction is already in the resistive state, and curve 3 is for the critical current of the bottom junction in the type 2 device. The second period in the curve 2 has not appeared due to the poor resolution of the automatic data acquisition system when tracing the maximum current of the resistive branches at small bias currents.

$T = 4.2$ K, at which the samples have been measured, $\Delta_{Ta} = 0.07$ meV (the value derived from the gap-difference feature in IVC; see Fig. 2), which is a small value as compared with $\Delta_{Ta}(T = 0) = 0.7$ meV, the London penetration depth $\lambda_{Ta}(T = 4.2\ \mathrm{K})$ is much larger than $\lambda_{Ta}(T = 0)$. It means that the system is in the high-T limit [10], in which the magnetic field penetrates deep into Ta, and screening currents only flow near the Ta/Nb interface. Therefore, the Ta layer produces a negligibly small screening effect and the bias current flows across it homogeneously, as it does in a normal metal.

Further evidence that both type 1 and type 2 devices are working in the lumped-junction regime comes from the $I_c(H)$ dependences. The magnetic field was applied in parallel to the junction plane. The dependences for the two devices (type 1 and type 2) are shown in Fig. 3. Curve 1 is the $I_c(H)$ dependence for the critical current at which the type 1 device switches to the resistive state, curve 2 is for the critical current of the single junction in the same device, when the second junction is already in the resistive state, and curve 3 is for the critical current of the bottom junction in the type 2 device. All the curves are symmetric with respect to the I_c axis, and reveal the shape characteristic of high-quality lumped junctions without any noticeable influence of the self-field effects. It is important that the curves 2 and 3 which represent the first period of the diffraction pattern are considerably wider than the first period of the pattern in curve 1, and approach the same value of the critical magnetic field at which the critical current first falls to zero. The last fact gives support to the assumption made in Ref. [3] that the curve 2 of the $I_c(H)$ dependence represents the $I_c(H)$ dependence of the single junction from the stack, as if the second junction, biased to the gaps-sum voltage, is not present. Since the size of the devices is small and high magnetic fields were required to trace several periods of the diffraction pattern, we could only measure the first period in this case. For the type 1 device working in the "single-junction" regime [3], the critical magnetic field is smaller (curve 1) than in the other two cases (curves 2 and 3).

The simplest and most straightforward assumption to explain an enhanced critical current in the type 1 devices is to consider the two barriers and the superconducting layer in between as a junction in parallel to the bottom and top junctions. Then we have an additional channel of Josephson tunneling and, in the case of identical junctions, can write the expression for the supercurrent through the device as

$$I = I_c \sin \varphi_{b,t} + I_p \sin(\varphi_b + \varphi_t),$$

where φ_b and φ_t are the phase differences across the bottom and top junction, respectively, I_p is the maximum critical current of the assumed junction connected in parallel. From the standard tunneling theory, one can estimate the magnitude of I_p as compared with I_c. Using, for example, the approach described in Ref. [12], we obtain the single-particle probability of order $\sigma \sim 10^{-5}$ for the junctions with the specific tunnel resistance of order $10^{-6}\ \Omega\ \mathrm{cm}^2$. The probability of Josephson tunneling is of the same order of magnitude [13]. Taking into account that in a simple model assumed above the tunneling through each of the two barriers in the stack is uncorrelated, the probability of simultaneous tunneling through the two barriers is the product of the probabilities for the single junctions, i.e. it is of order 10^{-10}. This implies that the magnitude of I_p should be of order $10^{-5} I_c$, which is much smaller

than the experimentally observed value $2 \times 10^{-2} I_c$. Therefore, the model cannot describe the phenomena.

Finally, we should analyze a possible influence of the proximity effect. One may argue that the middle Nb/Al layer in type 1 devices is proximitised through the tunnel barrier from the top by a different environment than in type 2 devices, which results in an induced superconductivity in the first case. An important parameter which defines the strength of the proximity effect is the coupling energy Γ_N [14]:

$$\Gamma_N = \frac{\hbar \nu_{FN} \sigma}{4 B d_N},$$

where ν_{FN} is the Fermi velocity in N metal (in our case, the middle Nb/Al layer with reduced superconductivity), d_N is the N thickness and B is a function of d_N and the mean free path, $B \sim 1$. With $\nu_{FN} \sim 1 \times 10^8$ cm/s and $d_N \sim 9$ nm for the intermediate layer, and $\sigma \sim 10^{-5}$, we obtain $\Gamma_N \approx 2 \times 10^{-4}$ meV. In fact, this gives the order of magnitude of the correction to the BCS energy gap of the intermediate electrode, induced by the proximity effect. It is obvious that such a small value cannot produce any noticeable change in the supercurrent through the tunnel barrier. An indirect indication of the negligible proximity effect through the tunnel barriers is the shape of the $I_c(T)$ dependence (Fig. 4). Near T_c of the middle layer, it does not display a positive curvature, unlike the dependence characteristic of the proximitised junctions [15].

One may suggest that the devices described here reveal a complicated nonlinear interaction between the junctions, which, however, is dependent on the barrier transparency. For comparison, we have fabricated devices from the similar structures, in which the critical current density j_c of the junctions is 10 times smaller than j_c of the junctions considered here. In this case, the difference between the critical currents of the type 1 device and the bottom junction of the type 2 device has not exceeded the spread of I_c of the type 1 devices within the array. We suppose that the observed phenomenon is a manifestation of a mesoscopic behavior of the system, in which the details of the device structure such as composition of the thin middle Nb/Al layer and the quality of interfaces between the layers play a role. A more detailed experimental and theoretical investigation of the system is necessary to establish the nature of the phenomena.

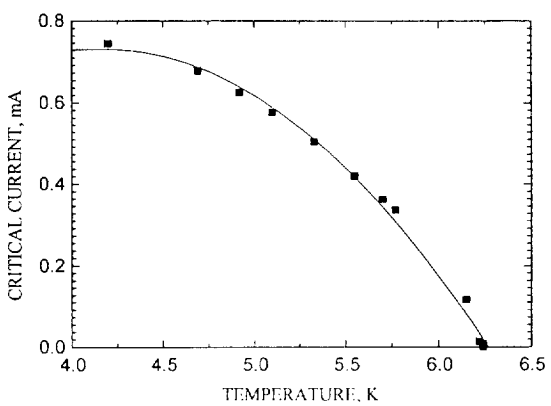

Fig. 4. The experimental $I_c(T)$ dependence for the Nb/Al–AlO_x–Nb/Al–AlO_x–Nb device (scatter plot). The solid line is the polynomial fit of the experimental points. The error bars are of the order of the symbol size.

Acknowledgement

The authors acknowledge stimulating discussions with A.V. Ustinov. This work is supported by the Royal Society and by INTAS grant No. 94-1783.

References

[1] S. Sakai, P. Bodin and N.F. Pedersen, J. Appl. Phys. 73 (1993) 2411.
[2] A.V. Ustinov, H. Kohlstedt, M. Cirillo, N.F. Pedersen, G. Hallmanns and C. Heiden, Phys. Rev. B 48 (1993) 10614.
[3] I.P. Nevirkovets, J.E. Evetts and M.G. Blamire, Phys. Lett. A 187 (1994) 119.
[4] R. Kleiner and P. Mueller, Phys. Rev. B 49 (1994) 1327.
[5] D.H. Kim, K.E. Gray and J.H. Kang, Phys. Rev. B 45 (1992) 7563.
[6] D.W. Jillie, J.E. Lukens, Y.-H. Kao and G.J. Dolan, Phys. Lett. A 55 (1976) 381.
[7] K.K. Likharev, Dynamics of Josephson junctions and circuits (Gordon and Breach, New York, 1986).
[8] H. Amin, M.G. Blamire, K.E. Page and J.E. Evetts, IEEE Trans. Magn. MAG-27 (1991) 3145.
[9] J.H. Claassen, J.E. Evetts, R.E. Somekh and Z.H. Barber, Phys. Rev. B 44 (1991) 9605.

[10] M.S. Pambianchi, J. Mao and S.M. Anlage, Phys. Rev. B 50 (1994) 13 659.
[11] G. Deutscher and P.B. de Gennes, in: Superconductivity, ed. R.D. Parks (Dekker, New York, 1969) p. 1005.
[12] E. Burstein and S. Lundqvist, eds., Tunneling phenomena in solids (Plenum Press, New York, 1969).
[13] B.D. Josephson, Rev. Mod. Phys. 36 (1964) 216.
[14] W.L. McMillan, Phys. Rev. 175 (1968) 537.
[15] L. Capogna and M.G. Blamire, Inst. Phys. Conf. Ser. No. 148 (1995) 1455.